Journal of Marine Research, 47, 111–130, 1989

Critical control of zonal jets by bottom topography

by Larry J. Pratt[1]

ABSTRACT

The nonlinear influence of isolated topography on an equivalent barotropic, quasigeostrophic jet is considered. The flow depends on several dimensional parameters including the mass flux Q, the mean layer thickness H, the planetary potential vorticity gradient β, the inertial boundary layer thickness $(u_0/\beta)^{1/2}$ and a parameter $a - c$ measuring the north-south potential vorticity difference across the jet. Eastward jets can achieve one of two steady forms, the first supercritical and the second subcritical with respect to upstream propagation of a long potential vorticity wave. An isolated topographic feature such as a ridge can cause the jet to undergo transition from subcritical to supercritical flow and thereby achieve a steady state analogous to hydraulically controlled open channel flow. In a critically-controlled state the values of Q, a-c, H, and $(u_0/\beta)^{1/2}$ cannot be specified independently of the topographic parameters and the topography thereby exerts an 'upstream influence' which is felt by the general circulation of the ocean as a whole. Critically-controlled states also experience topographic form drag, whereas noncontrolled states experience none. The form drag is determined by the upstream potential vorticity distribution of the flow and the critical jet width, suggesting that this type of drag might be estimated in practice by a combination of hydrographic data and satellite imagery. The Antarctic Circumpolar Current is discussed as a possible example.

1. Introduction

The surface of the earth and ocean bottom are marked by numerous mountain ranges, ridges, and seamount chains which exercise various degrees of influence on the atmospheric and oceanic circulation. A fundamental question is whether this influence is purely local in nature, involving disturbances which are confined to the immediate vicinity of the topographic feature, or whether the influence can be felt throughout the general circulation as a whole. This paper discusses one mechanism, namely critical control or 'upstream influence' by which a global influence can be exercised. The mechanism involves potential vorticity wave dynamics and applies over horizontal scales much larger than those associated with the familiar critically-controlled, gravitationally-driven flows of classical hydraulics.

The calculations presented herein are motivated by the work of Armi (1974, 1989a, b) showing that an eastward jet, separated from the (motionless) far field by shear layers, can possess two forms or 'conjugate states' for a given flow rate and total

1. Woods Hole Oceanographic Institution, Woods Hole, Massachusetts, 02543, U.S.A.

energy. When the parameter $U/\beta a^2 = 1$ the conjugate states are identical. (U is the maximum velocity, a is the jet half-width, and β is the planetary potential vorticity gradient.) The flow is thereby analogous to open channel flow where two conjugate states, one subcritical and the other supercritical with respect to long gravity waves, arise for a given flow rate and Bernoulli function. When the Froude number of the flow is unity, the conjugate states are identical and the flow is critical, as at a point of hydraulic control. Armi (1989a) is able to establish a critically-controlled jet by circulating fluid through a rotating laboratory annulus and observing that $U/\beta a^2 = 1$ near the point of withdrawal and <1 upstream.

These findings suggest that oceanic and atmospheric jets might be subject to critical control by topographic features such as ridges and mountain ranges. The purpose here is to place this idea on firmer ground by presenting a deductive model describing the nonlinear influence of bottom topography on an idealized, quasigeostrophic jet. The calculations herein differ from those of Armi (1974, 1989a, b) in the following respects: First, topography is explicitly included, allowing computation of the along-stream structure of the jet as it flows over ridges or seamounts. Second, it is shown by direct calculation that long waves are stationary (the flow is critical) at the point of merger of conjugate states. Finally, potential vorticity is conserved along all stream lines, whereas this is not necessarily true in Armi's calculations.

The solution technique employed is similar to that used by Fofonoff (1954) in his discussion of free inertial modes in closed basins and Charney (1955) in his inertial model of the Gulf Stream. Specifically, the geostrophic potential vorticity equation for a constant density layer is integrated by specifying potential vorticity along stream lines in accordance with an assumed upstream distribution. The functional relationship used by these authors is enriched here by introducing potential vorticity fronts, allowing a jet-like velocity distribution. Section 2 describes the jet-like flow that forms when two potential vorticity fronts separated by a distance ΔL are present. In Section 3 a critical condition for the jet is established by calculating the value of ΔL at which long waves become stationary. The next section details a specific calculation describing the interaction of the jet with a ridge and the corresponding conjugate states. It is shown that critically-controlled states can occur, with subcritical flow upstream and supercritical flow downstream of the ridge, provided that certain necessary conditions are met. Among these are, first, the mass flux between the fronts must be eastward; second, the ridge elevation must equal or exceed a certain minimum value at the crossing point of the jet; and third, the ridge elevation must vary in the longitudinal (or cross stream) direction. The form drag exerted against the critically-controlled flow by the ridge is calculated. Finally, Section 5 discusses the Antarctic Circumpolar Current (ACC) as a possible example of a critically-controlled, jet-like flow. Specifically, I point out that the geometry of the dynamic height contours near topographic feature such as the Kerguelen Plateau, Macquarie Ridge and possibly the Drake Passage resemble the streamline patterns characteristic of a critically-controlled flow. In

addition, estimates of an appropriately defined Froude number at and upstream of Drake Passage give the magnitudes required for critical control.

At this point it is instructive to review the reasoning behind the expectation that critically-controlled states will arise in nature. Consider the effect of suddenly removing a barrier at $x = 0$ which dams a reservoir of resting, nonrotating fluid occupying $x < 0$. Under the influence of gravity the fluid will accelerate and spill outward to fill the void. This acceleration ceases, however, when the flow reaches the critical speed at some location, in this case $x = 0$. At this point in time, signals from downstream can no longer propagate back into the reservoir and the fluid there lacks information that would trigger further time-dependent adjustment. (The solution to this problem is described in Stoker, 1957.) In summary, the signal propagation which triggers time-dependent adjustment favors the establishment of a flow with supercritical flow downstream and subcritical flow upstream of some 'control point'. Parallel processes act in many other types of fluid systems, providing a strong precedent for larger scale geophysical flows. In fact, Gill and Schuman (1979), Hughes (1985, 1986, 1987), and Luyten and Stommel (1985) have suggested that oceanic boundary currents such as the Gulf Stream and Agulhas can be critically-controlled. Hughes (1979, 1981) has also identified multiple conjugate states in models of the equatorial undercurrent.

Finally, it should be noted that many previous analytical studies of nonlinear flow over isolated, mesoscale topography [e.g. Pierrehumbert (1985), Pierrehumbert and Wyman (1985), Merkine (1975), Jacobs (1964), and Robinson (1960)] assume uniform potential vorticity. Upstream effects due to the topography *can* be transmitted by internal gravity waves, but the spatial extent of these effects tends to be limited by rotation (Pierrehumbert and Wyman, 1985). Topographically forced flows with finite potential vorticity gradients have also been treated [e.g. Porter and Rattray (1964), McIntyre (1986), Clark and Fofonoff (1969), McCartney (1976), and Davey (1980)]. In all cases the flow is assumed to be initially uniform or uniform far upstream of the topographic feature and topographic effects are confined to the immediate vicinity or the lee of this feature. Only in cases of periodic upstream and downstream boundary conditions are permanent disturbances observed upstream of the topography. The novelty of the present model rests in the jet-like velocity distribution imposed upstream of the topography. Jets give rise to wave modes not present in uniform flows and it is well known, for example, that symmetric jets allow symmetric (or varicose) modes. These modes are associated with widening and narrowing (rather than meandering) of the jet and are solely responsible for upstream influence in the present problem.

2. The model

The starting point of the investigation is the steady quasigeostrophic potential vorticity equation for a single layer (or equivalent barotropic, two layer) ocean or

atmosphere. Following the notation of Pedlosky (1987, Eq. 3.13.4) this equation can be written

$$\nabla^2\psi - F\psi + \eta_B + \beta y = G(\psi) \tag{2.1}$$

where

$$\nabla^2 = \frac{\partial^2}{\partial x^2} + \frac{\partial^2}{\partial y^2}$$

$\psi = \eta^*/\epsilon FH$ (the dimensionless stream function)

$\eta_B = \eta_B^*/\epsilon H$ (the dimensionless bottom elevation)

$\beta = \beta^* L^2/U$ (the dimensionless planetary potential vorticity gradient)

$(x, y) = (x^*, y^*)L$ (the dimensionless eastward and northward cartesian coordinates)

$(u, v) = (u^*, v^*)U$ (the dimensionless eastward and northward velocities)

and $G(\psi)$ represents the dimensionless potential vorticity. The dimensional scales U, L, and H represent typical horizonal velocity, horizontal length, and layer depth, and g and f are the gravitational acceleration and Coriolis parameter. The dimensional variable η^* represents the free surface elevation or, in the case of an equivalent barotropic lower layer, the interfacial elevation. The Rossby number $\epsilon = U/fL$ is $\ll 1$ in the quasigeostrophic approximation whereas $F = f^2 L^2/gH$ will remain arbitrary.

The bottom elevation is assumed to have the separable form

$$\eta_B = \mathcal{N}(x)S(y)$$

with $\mathcal{N}(x) \to 0$ as $|x| \to \infty$, as for an isolated bump or ridge. With this choice (2.1) becomes

$$\nabla^2\psi + \mathcal{N}(x)S(y) + \beta y = G(\psi) + F\psi. \tag{2.2}$$

I also assume that the potential vorticity $G(\psi)$ is determined by processes occurring far upstream of the topography which are not explicit in the present model. Therefore, one may pre-specify $G(\psi)$ and calculate the resulting flow for various topographies by solving (2.2). Here, the pre-specification is based on the requirement that the flow be jet-like and nearly zonal. Hence, I require that $u = -u_0$ and $v = 0$ as $|y| \to \infty$ and $|x| \to \infty$ (i.e. away from the core of the jet and the topography). Setting $\mathcal{N} = \nabla^2\psi = 0$ in (2.2) leads to

$$\beta y = G(\psi) + F\psi$$

and differentiating this expression with respect to y gives

$$-G'(\psi) = -(\beta/u_0) + F.$$

The first requirement then is that $G'(\psi)$ approach a constant value[2] away from the jet and the topography.

The choice of $G(\psi)$ within the core of the jet can be motivated by noting that zonal jets like the Gulf Stream east of Hatteras possess intrinsic potential vorticity gradients much stronger than β^*. For example, Hall (1985) shows that the maximum potential vorticity gradient in the upper Gulf Stream near 68W is approximately 50 times larger than the planetary potential vorticity gradient. These strong features are a consequence of the funneling effect of major zonal jets whereby fluid parcels originating from widely separated latitudes can be brought into close proximity. In the present model I attempt to mimic these local gradients by introducing discontinuities in the value of G across certain streamlines. Specifically:

$$G(\psi) = [(\beta/u_0) - F]\psi + \delta[y; L_1(x), L_2(x)] \tag{2.3}$$

where

$$\delta = \begin{cases} a & y > L_1(x) \\ b & L_2(x) < y < L_1(x) \\ c & y < L_2(x) \end{cases}$$

The flow is thus divided into three regions (I, II and III), each containing the same potential vorticity gradient but each having a different 'background' potential vorticity ($= a$, b, or c). The regions are separated by potential vorticity fronts coinciding with the streamlines at $y = L_1(x)$ and $y = L_2(x)$ across which $G(\psi)$ is discontinuous, but u, v, and ψ are continuous. A definition sketch is shown in Figure 1.

It is further assumed that the topography and flow have a 'long wave' character, meaning that the scale of variation L in the x-direction is always much greater than the y-scales $L_1 - L_2$, $\sqrt{gH}/f$, etc., and that the x-velocity scale is much larger than the y-velocity scale. Denoting by ϵ a typical ratio of the former to the latter, the continuity equation ($\partial u/\partial x + \partial v/\partial y = 0$) suggests that v should typically be smaller than u by a factor ϵ. The relative vorticity term $\partial v/\partial x$ is therefore smaller than $\partial u/\partial y$ by a factor ϵ^2, and $\nabla^2\psi$ may be replaced by $\psi_{yy} + 0(\epsilon^2)$. Doing so in (2.2) and substituting (2.3) for $G(\psi)$ leads to the approximate equation

$$\psi_{yy} - \alpha^2\psi = -\beta y - \mathcal{N}(x)S(y) + \delta(y; L_1(x), L_2(x)) \tag{2.4}$$

where

$$\alpha^2 = \beta/u_0.$$

2. This argument is equivalent to those used by Fofonoff (1954) in his discussion of free inertial modes in closed basins and by Charney (1955) in his model of the Gulf Stream. Both use constant $G'(\psi)$.

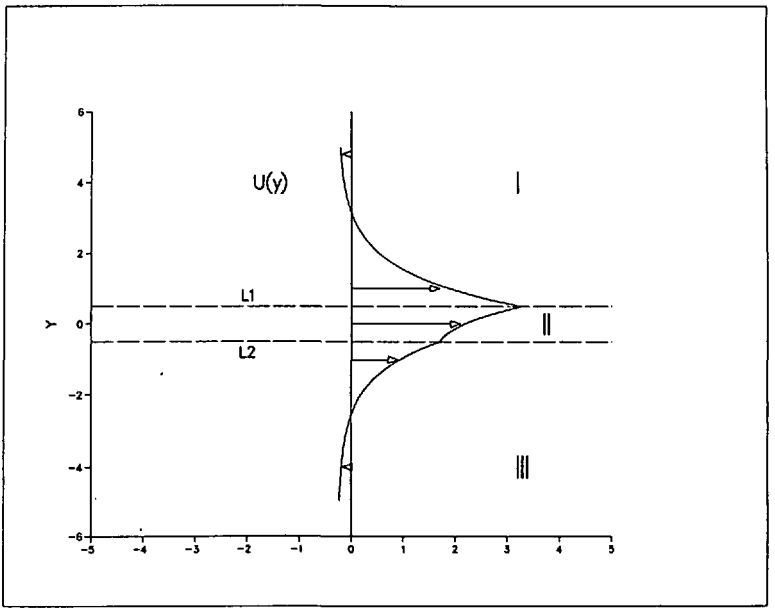

Figure 1. Definition sketch showing potential vorticity fronts at $y = L_1$ and $y = L_2$ and velocity profile for the case $\alpha = 1$, $a - b = 6.5$, $b - c = 1.5$, $\beta = .25$, and $\mathcal{N} = 0$. The abscissa represents both the x-axis and the velocity scale.

As will be seen presently, the long wave approximation eliminates wave dispersion and therefore expunges lee waves from the problem.

It is assumed that all steady flows have been established as the result of adjustment from some simple initial state having continuous velocity. Conservation of potential vorticity then implies that the velocity remains continuous at all times and this is used as the matching condition across the two fronts. This condition is uneffected by the long wave approximation. The solution to (2.4) satisfying the condition of velocity continuity and for which ψ remains bounded as $|y| \to \infty$ is

$$\psi = \begin{cases} (2\alpha^2)^{-1}[(b-c)e^{-\alpha\Delta L} + (a-b)]e^{-\alpha(y-L_1)} + \alpha^{-2}[\beta y + \mathcal{N}D - a] & (y > L_1) \\ (2\alpha^2)^{-1}[(b-a)e^{-\alpha(L_1-y)} + (b-c)e^{-\alpha(y-L_2)}] + \alpha^{-2}[\beta y + \mathcal{N}D - b] & (L_2 < y < L_1) \\ (2\alpha^2)^{-1}[(b-a)e^{-\alpha\Delta L} + (c-b)]e^{-\alpha(L_2-y)} + \alpha^{-2}[\beta y + \mathcal{N}D - c] & (y < L_2) \end{cases} \quad (2.5)$$

where $\Delta L(x) = L_1 - L_2$ and $D(y)$ satisfies

$$D_{yy} - \alpha^2 D = -\alpha^2 S(y). \quad (2.6)$$

The horizontal velocities are

$$u = -\psi_y = (2\alpha)^{-1}\left[(a-b)e^{-\alpha|y-L_1|} + (b-c)e^{-\alpha|y-L_2|}\right] - u_0 - \alpha^{-2}\mathcal{N}D' \quad (2.7a)$$

$$v = \psi_x = (2\alpha)^{-1}\left[(a-b)e^{-\alpha|y-L_1|}\partial L_1/\partial x + (b-c)e^{-\alpha|y-L_2|}\partial L_2/\partial x\right] - \alpha^{-2}\mathcal{N}'D. \quad (2.7b)$$

Eq. (2.7a) shows that the zonal velocity is composed of a westward background component u_0, a component related to the y-variation of the topography and two components which decay away from the potential vorticity fronts. The latter are proportional to the potential vorticity jumps across the fronts. The decay scale $\alpha^{-1} = (u_0/\beta)^{1/2}$ is identical to the inertial boundary layer thickness in the Fofonoff (1954) and Charney (1955) problems. Figure 1 shows a sample velocity profile for a purely zonal flow ($\mathcal{N} = 0$) with $\beta = .25$, $\alpha = 1$, $(a-b) = 6.5$, and $(b-c) = 1.5$.

3. Critical flow

Steady flows such as that of Figure 1 are able to support linear wave modes due to the presence of the restoring mechanisms associated with the β-effect and the potential vorticity jumps. I now attempt to identify conditions under which the phase speed $\tilde{c}$ of any long wave mode vanishes. Consider a small perturbation $\psi' = Re[A\, e^{ik(x-\tilde{c}t)}]$ of a basic state described by $\psi = \bar{\psi}$. Although long wavelengths are assumed, the topographic term $\mathcal{N}(x)$ is assumed to vary on an even longer scale, so that the x-dependence of $\bar{\psi}$ and $\mathcal{N}$ is merely parametric. Substituting $\psi = \bar{\psi} + \psi'$ into the time-dependent quasigeostrophic potential vorticity equation, linearizing, and neglecting $O(k^2)$ terms leads to

$$(\bar{U}(y) - \tilde{c})(d^2A/dy^2 - FA) + (\beta + \mathcal{N}D' + F\bar{U} - d^2\bar{U}/dy^2)A = 0 \quad (3.1)$$

where $\bar{U} = -d\bar{\psi}/dy$ (cf. Eq. 7.14.b in Pedlosky, 1987). Away from the potential vorticity fronts the basic potential vorticity gradient is given by

$$dG/dy = (\beta + \mathcal{N}D' + F\bar{U} - \bar{U}_{yy}) = (\alpha^2 - F)\bar{U} \quad (3.2)$$

in view of (2.1). Combining (3.1) and (3.2) leads to the alternative normal mode equation

$$d^2A/dy^2 - [F + (\alpha^2 - F)\bar{U}/(\bar{U} - \tilde{c})]A = 0. \quad (3.3)$$

At the potential vorticity fronts I demand that A be continuous, leading to the linearized matching condition

$$[A]^+_- = 0 \qquad (y = L_1, L_2) \quad (3.4)$$

where $[V]^+_-$ denotes $V(y^+) - V(y^-)$ at the designated values of y, and L_1 and L_2 may be regarded as the positions of the potential vorticity fronts in the basic state.

Integration of (3.1) across each front and use of (2.3) and (3.2) then gives the additional matching conditions

$$[\bar{U} - \tilde{c}][dA/dy]_-^+ + (a - b)A = 0 \qquad (y = L_1) \tag{3.5a}$$

$$[\bar{U} - \tilde{c}][dA/dy]_-^+ + (b - c)A = 0 \qquad (y = L_2) \tag{3.5b}$$

The object now is to search for a basic state such that $\tilde{c} = 0$ is an eigenvalue of (3.3)–(3.5). Setting $\tilde{c} = 0$ in (3.3) leads to $d^2A/dy^2 - \alpha^2 A = 0$, and the solution which decays at $|y| = \infty$ and satisifes (3.4) can be written

$$A = \begin{cases} (C_1 + C_2 e^{\alpha\Delta L}) e^{-\alpha(y - L_1)} & (y > L_1) \\ C_1 e^{-\alpha(y - L_1)} + C_2 e^{\alpha(y - L_2)} & (L_1 > y > L_2) \\ (C_1 e^{\alpha\Delta L} + C_2) e^{\alpha(y - L_2)} & (y < L_2) \end{cases} \tag{3.6}$$

Applying (3.5 a, b) with $\tilde{c} = 0$ leads to

$$\begin{aligned} (a - b)C_1 + [(a - b) - 2\alpha\bar{U}(L_1)]e^{\alpha\Delta L}C_2 &= 0 \\ [(b - c) - 2\alpha\bar{U}(L_2)]e^{\alpha\Delta L}C_1 + (b - c)C_2 &= 0. \end{aligned} \tag{3.7}$$

To obtain nontrivial solutions the determinant of the coefficients of C_1 and C_2 must be set to zero. Doing so and substituting for $\bar{U}$ using (2.7a) leads to the following condition for stationary waves:

$$\begin{aligned} 2\alpha^{-1}[\beta + \mathcal{N}_c D'(L_{1c})][\beta + \mathcal{N}_c D'(L_{2c})] \\ = \{(b - c)[\beta + \mathcal{N}_c D'(L_{2c})] + (a - b)[\beta + \mathcal{N}_c D'(L_{1c})]\} e^{-\alpha\Delta L_c}. \end{aligned} \tag{3.8}$$

The subscript c is used to denote 'critical' values of the variables, i.e., those values at which the linear phase speed is zero. This usage should not be confused with the usage common in instability theory where 'critical' refers to a stability threshold.

4. Critically-controlled states

There are a number of ways of representing the steady states possible for given topography. One of the most instinctive representations is in terms of the flow rate Q in Region II:

$$Q = \int_{L_1}^{L_2} u\, dy = \alpha^{-2}\left\{\frac{1}{2}(a - c)(1 - e^{-\alpha\Delta L}) - \beta\Delta L - \mathcal{N}[D(L_1) - D(L_2)]\right\} \tag{4.1}$$

in view of (2.7a). I will call flows having $Q > 0$ eastward jets and flows having $Q < 0$ westward jets.

Now consider the example of flow over an isolated ridge with elevation which increases linearly in the y-direction: $S = S_0 + sy$. From (2.6) the corresponding forcing

term is $D(y) = S_0 + sy$ and substitution in (4.1) leads to the following single equation for $\Delta L(x)$:

$$s\mathcal{N} = \frac{\frac{1}{2}(a - c)(1 - e^{-\alpha\Delta L}) - \beta\Delta L - \alpha^2 Q}{\Delta L}. \tag{4.2}$$

For each value of the topographic parameter $s\mathcal{N}$, (4.2) determines (possibly many) values of the jet 'width' ΔL. In physical terms, $s\mathcal{N}$ is the northward slope of the topography and is therefore a measure of the topographic potential vorticity gradient. As a fluid parcel passes the ridge, it experiences a changing ambient potential vorticity gradient due to the variations in $s\mathcal{N}$, forcing ΔL to change.

The critical condition (3.8) reduces to

$$2(\beta + \mathcal{N}_c s)/\alpha (a - c) = e^{-\alpha\Delta L_c} \tag{4.3}$$

for the present choice of topography. Critical flow can thus exist if an ambient potential vorticity gradient exists as provided by β or the bottom slope s. In addition, the ambient potential vorticity gradient must be smaller in magnitude and of the same sign as the equivalent intrinsic potential vorticity 'gradient' $\alpha(a - c)/2$; that is,

$$0 \leq 2(\beta + \mathcal{N}_c S)/\alpha (a - c) \leq 1.$$

In dimensional terms, this requirement can be written

$$0 \leq \frac{2(u_0^*/\beta^*)^{1/2}\,[\beta^* + f\partial(\eta_B^*/H)_c/\partial y^*]}{H(a^* - c^*)} \leq 1 \tag{4.4}$$

where the star superscript denotes dimensional versions of previously-defined quantities.

The simplest way to illustrate the dependence of ΔL upon $\mathcal{N}$ is to plot the right-hand side of (4.2) and locate its intersections with the horizontal line $s\mathcal{N}$, as done in Figure 2. Note that

$$s\mathcal{N}'(\Delta L) = (\Delta L)^{-2}\{\alpha^2 Q - \tfrac{1}{2}(a - c)[1 - (1 + \alpha\Delta L)e^{-\alpha\Delta L}]\}$$

so that extrema occur when

$$\frac{2\,\alpha^2 Q}{(a - c)} = 1 - (1 + \alpha\Delta L)e^{-\alpha\Delta L} \qquad (\mathcal{N}'(\Delta L) = 0) \tag{4.5}$$

Elimination of Q between (4.2) and (4.5) leads to an expression for the value of $s\mathcal{N}$ at the extrema:

$$s\mathcal{N}_c = \tfrac{1}{2}\alpha(a - c)e^{-\alpha\Delta L_c} - \beta. \tag{4.6}$$

Comparison with (4.3) shows that (4.6) is just the critical condition for ΔL, and the

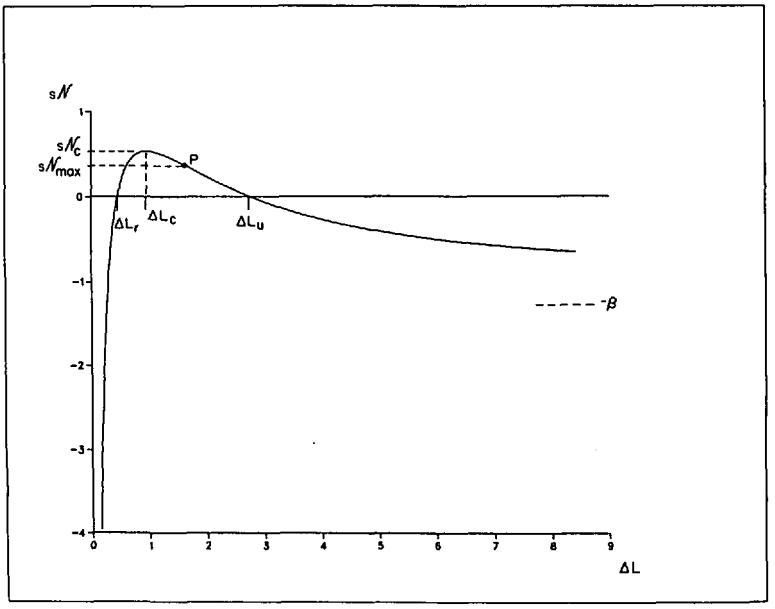

Figure 2. Solution curve showing $s\mathcal{N}$ as function of ΔL for $Q = \alpha = \beta = 1, a - c = 8$.

subscript c has been introduced accordingly. Thus, extrema in the $s\mathcal{N}(\Delta L)$ curve occur when the flow is critical.

The right-hand side of (4.5) increases monotonically from zero to unity as ΔL goes from zero to ∞ and therefore one critical value of ΔL exists provided that

$$0 \leq \frac{2\alpha^2 Q}{(a-c)} \leq 1,$$

otherwise critical flow is not possible. In dimensional terms the above requirement can be written

$$0 \leq \frac{2Q^*}{H^2(u_0^*/\beta^*)(a^* - c^*)} \leq 1 \tag{4.7}$$

where Q^* is the dimensional volumetric flow rate. It will be shown later that (4.7) is a necessary condition for the existence of *any* solution, controlled or otherwise. The physical interpretation is that the geostrophic mass flux cannot exceed a value determined by the difference in layer depth across the jet implicit in the potential vorticity difference.

If one further observes from (4.2) that $s\mathcal{N}(\Delta L) \to -\infty$ as $\Delta L \to 0$ and $s\mathcal{N}(\Delta L) \to -\beta$ as $\Delta L \to \infty$, then the salient characteristics of the solution curve are known. Figure 2 shows the solution curve for the case $Q = 1, \alpha = 1, (a - c) = 8, \beta = 1$. The curve has a single maximum at $\Delta L_c = .96$ and $s\mathcal{N}_c = 0.53$. I will refer to flows having

$\Delta L < \Delta L_c$ as supercritical and those having $\Delta L > \Delta L_c$ as subcritical in the anticipation that only the latter will permit upstream propagation of the controlling linear wave mode. This hypothesis is based on the simple observation that smaller values of ΔL must correspond to larger mean eastward velocities in order to conserve the flow rate Q. Thus, the eastward advective tendency grows as the ΔL decreases. In addition, the subcritical states observed in the Armi (1989a) experiment corresponded to widths greater than the critical width. These considerations suggest categorization of the flow according to a β – Froude number (or 'Froude/Rossby number,' as labeled by Armi, 1989a), defined by

$$F_\beta = \frac{\alpha(a - c)e^{-\alpha\Delta L}}{2(\beta + s\mathcal{N})} = \frac{H(a^* - c^*)e^{-\Delta L^*/(u_0^*/\beta^*)^{1/2}}}{2(u_0^*/\beta^*)^{1/2}\,[\beta^* + f\partial(\eta^*/H)/\partial y^*]}. \tag{4.8}$$

The flow is thus supercritical, subcritical or critical according as $F_\beta > 1$, $F_\beta < 1$, or $F_\beta = 1$.

The two values of ΔL or 'conjugate states' corresponding to flow far away from the topography lie at the two intersections of the solution curve with the $s\mathcal{N} = 0$ axis. In Figure 2, the subcritical value has been labeled ΔL_u and the supercritical value ΔL_r. In order for these solutions to exist at all, the solution curve must have a maximum (already guaranteed by 4.7) lying above the ΔL axis, i.e. $s\mathcal{N}_c$ must be positive. According to (4.6) this requirement is equivalent to $\alpha(a - b)e^{-\alpha\Delta L_c} > 2\beta$ which, in turn, can be satisfied only if $\alpha(a - b) > 2\beta$, or

$$\frac{2(u_0^*/\beta^*)^{1/2}}{H(a^* - b^*)}\beta^* < 1. \tag{4.9}$$

In summary (4.7) and (4.9) may be regarded as necessary conditions for the existence of the eastward flowing jet, controlled or otherwise.

Now suppose that the upstream flow is subcritical, $\Delta L = \Delta L_u$, and that the topography consists of an isolatged ridge with $\mathcal{N}_{\max}$ less than $\mathcal{N}_c$. An observer approaching the ridge from the west will see that ΔL decreases from ΔL_u as $\mathcal{N}(x)$ begins to increase. When the crest of the ridge is met (point P in Fig. 2) ΔL has reached its minimum value; proceeding farther east causes ΔL to increase until the value ΔL_u is reached. In this subcritical solution the upstream and downstream values of ΔL are identical. A similar scenario is possible when the upstream flow is supercritical ($\Delta L = \Delta L_r$) with ΔL initially increasing, then decreasing to its upstream value as the ridge is passed.

If $\mathcal{N}_c = \mathcal{N}_{\max}$, ΔL can pass from the subcritical to supercritical branch of the solution curve or vice versa. When the upstream state is subcritical, $\Delta L = \Delta L_u$, the jet width decreases continuously as the topography is passed and $\Delta L \to \Delta L_r$ far downstream. In this state upstream wave propagation is allowed upstream but not downstream of the ridge crest, and the flow is critically-controlled. The opposite case (supercritical flow upstream and subcritical downstream) is also possible; however, this arrangement in

the hydraulic analog is unstable at the crest of the obstacle.[3] In the present model it is expected that the expansion from supercritical to subcritical flow will involve some turbulent or wave-like transition analogous to a hydraulic jump.

A topographic depression ($\mathcal{N} < 0$) with a southward slope ($s < 0$) can also exert critical control in the manner described above. However, if $\mathcal{N}$ and s have opposite signs, as in a northward sloping trough, ΔL must lie outside the interval $\Delta L_r < \Delta L < \Delta L_u$ and no critical control is possible. Also if the topography has no y-structure ($s = 0$) then ΔL remains fixed at its upstream value ΔL_u or ΔL_r for all x and critical control is expunged. The physical interpretation is that the topography is no longer able to alter the ambient potential vorticity gradient and thereby induce the varicose changes necessary to achieve the desired critical width. In summary, it is necessary that

$$s\mathcal{N}_{\max} > 0 \tag{4.10}$$

for critical control.

If the flow is westward ($Q < 0$ for $\beta > 0$) then the solution curve in Figure 2 asymptotes to positive $s\mathcal{N}$ as $\Delta L \to 0$. Since the curve possesses at most one extremum it can cross the ΔL axis only once in this case. Hence, the upstream and downstream values of ΔL are always identical and no critical control is possible. In this case (or the case $s\mathcal{N}_{\max} < 0$, $Q > 0$) an apparent example of complete flow blockage can be found. Consider the case ($s\mathcal{N}_{\max} < 0$, $Q > 0$) and suppose that the upstream value of ΔL is subcritical and that $-s\mathcal{N}_{\max} > \beta$. To construct a solution over the topography one follows the solution curve (Fig. 2) to the right of ΔL_u. As $-s\mathcal{N}$ increases so does ΔL until the value $-s\mathcal{N} = \beta$ is reached, at which point ΔL becomes infinite. The physical explanation is that the total ambient northward potential vorticity gradient vanishes and the fronts turn and move along lines of constant eastward potential vorticity gradient. This description is somewhat speculative, however, since the long wave approximation is violated where $\Delta L \to \infty$.

Once $\Delta L(x)$ is determined the individual frontal positions $L_1(x)$ and $L_2(x)$ can be computed from $L_1 = L_2 + \Delta L$ and

$$L_2 = (\beta + \mathcal{N}s)^{-1}[\beta L_2(-\infty) - \mathcal{N}S_0 + \tfrac{1}{2}(a - b)(e^{-\alpha\Delta L} - e^{-\alpha\Delta L(-\infty)})].$$

The latter is obtained by evaluating (2.5) at $y = L_2$. Note that even when ΔL remains constant, as in the case of a uniform ridge, deflections of the fronts occur (L_1 and L_2 change) as the topography is crossed. Figure 3 shows examples of the solution types discussed above for parameter settings close to those of Figure 2 and for $\mathcal{N}(x) = \mathcal{N}_{\max}e^{-x^2}$.

3. As noted by Pratt (1984), wave propagation in this case is directed toward the ridge crest from upstream and downstream. Therefore, disturbances to the flow become focused at the crest and attain infinite energy density.

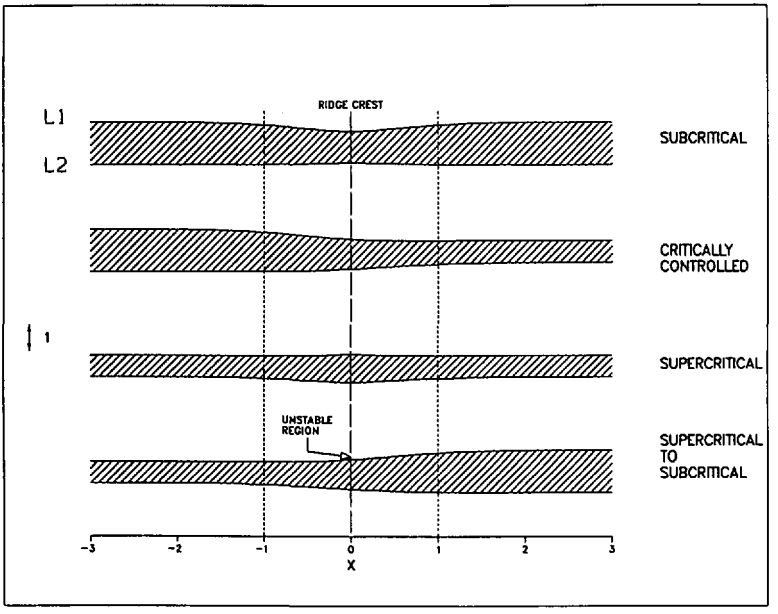

Figure 3. Examples of the four solution types for $\alpha = \beta = s = S_0 = 1, a - c = 6.5, b - c = 1$ and $\mathcal{N} = \mathcal{N}_{max} \exp(-x^2)$. $\mathcal{N}_{max}$ has value .0164 (subcritical); .0622 (critically-controlled); .0610 (supercritical); and .0622 (supercritical to subcritical). In all cases $L_2 = 0$ at $x = -\infty$ and the flow is from left to right.

If $\mathcal{N}_{max} > \mathcal{N}_c$ the flow cannot surmount the ridge. In classical hydraulics a similar situation can arise and there the flow undergoes a time-dependent adjustment in which new upstream conditions are established allowing passage of the fluid. The new steady state is critically-controlled and the time-dependent adjustment by which it is established essentially describes the process of upstream influence (see Baines and Davies, 1980, for a review of the subject). Solution of the corresponding time-dependent problem for the jet is not attempted here; however, it is anticipated that ridges with $\mathcal{N}_{max} > \mathcal{N}_c$ would induce adjustment to critically-controlled states.

It is also instructive to examine the case of a jet imbedded in a *resting* ocean. To understand this case in the context of the present model it should first be noted that the finite far field velocity, u_0, is intimately related to the β-effect. Since the potential vorticity is a function of ψ, the latter must vary in the far field to allow G to vary. Thus, taking $u_0 \to 0$ also requires $\beta \to 0$. Reformulation of the problem in this double limit results in a solution of the form (4.2), but with β/U_0 replaced by F and β (appearing alone) set to zero. The solution curve resembles the curve of Figure 2, but with $s\mathcal{N} \to 0$ as $\Delta L \to \infty$ and a single zero crossing at finite ΔL corresponding to supercritical flow. If $\mathcal{N}_{max}$ is less than $\mathcal{N}_c$ the solution resembles the supercritical flow of Figure 3. If $\mathcal{N}_{max} = \mathcal{N}_c$ the solution near the obstacle crest is unstable, as in the lower solution of Figure 3.

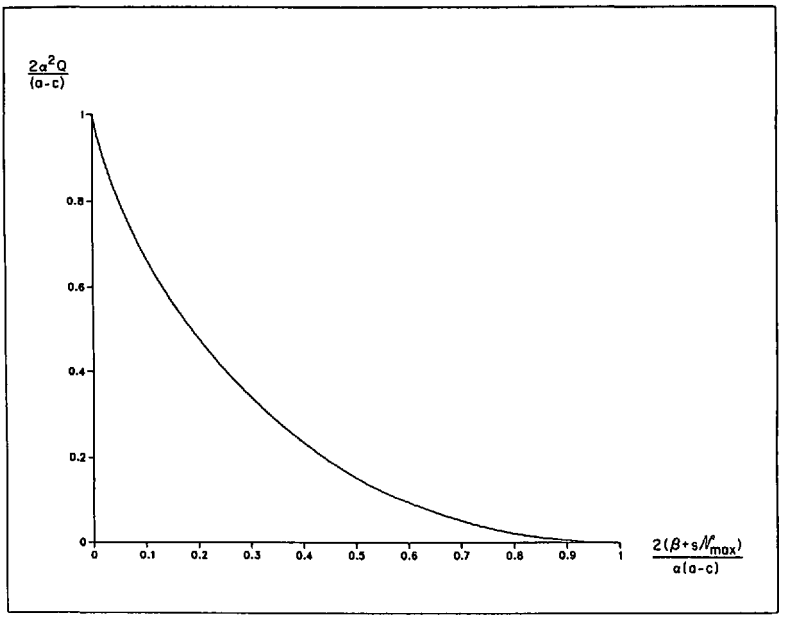

Figure 4. Flow rate as a function of the maximum ambient potential vorticity gradient for a critically-controlled jet. Q is the dimensionless flow rate per unit depth between the potential vorticity fronts and $s\mathcal{N}_{max}$ is the northward slope at the ridge crest. In dimensional terms the ordinate is $2Q^*/H^2(u_0^*/\beta^*)(a^* - c^*)$ and the abscissa is $2(u_0^*/\beta^*)[\beta^* + f\partial(\eta_B^*/H)/\partial y^*]/H(a^* - c^*)$.

Critical control implies a relationship between the elevation of the ridge and the flow rate, obtained by eliminating ΔL between (4.5) and (4.6):

$$\frac{2\alpha^2 Q}{(a-c)} = 1 + \left\{\ln\left[\frac{2(\beta + s\mathcal{N}_{max})}{\alpha(a-c)}\right] - 1\right\}\frac{2(\beta + s\mathcal{N}_{max})}{\alpha(a-c)}. \tag{4.11}$$

Figure 4 shows a plot of $2\alpha^2 Q/(a-c)$ vs. $2(\beta + s\mathcal{N}_{max})/\alpha(a-c)$ over the range in which critical control is possible (see 4.7 and 4.9). Increasing values of $s\mathcal{N}_{max}$ are associated with decreasing values of Q, and when $s\mathcal{N}_{max}$ exceeds the value $\frac{1}{2}\alpha(a-c) - \beta$ the flow becomes completely blocked ($Q = 0$). Eq. (4.3) shows that $\Delta L \to \infty$ in this case, implying that the fluid is forced to turn and flow parallel to the ridge, a situation which cannot be portrayed by long wave theory.

Two cases of apparent flow blockage by the topography have been noted. The first involves subcritical flow with $s\mathcal{N} < 0$, the blockage occurring when the ambient potential vorticity gradient $s\mathcal{N} + \beta$ vanishes. The second instance involves a critically-controlled flow with $s\mathcal{N} > 0$. If $s\mathcal{N}_c$ is increased to the point where the northward ambient potential vorticity gradient $s\mathcal{N}_c + \beta$ equals the northward intrinsic potential vorticity 'gradient' $\alpha(a-c)/2$, then $Q \to 0$. Finally, note that critically-controlled solutions experience a finite form drag due to the ridge, whereas the purely

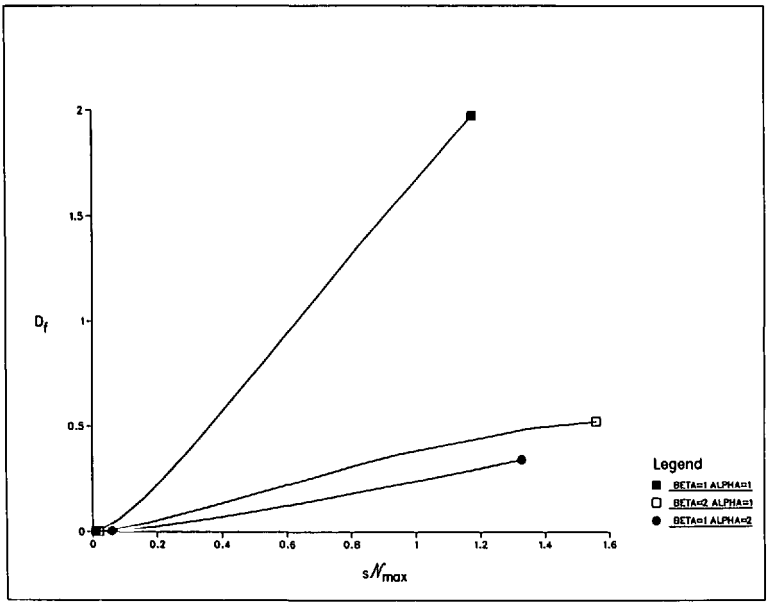

Figure 5. Form drag exerted by the ridge against the jet. For $a - b = 7$, $b - c = S_0 = s = 1$ and $L_1(-\infty) = 0$. Values of β and α are given in the legend.

subcritical or supercritical solutions experience none. Form drag refers to the net bottom pressure force exerted by the ridge against the flow (i.e. the integral of bottom pressure times the x-component of bottom slope over the area of the ridge). The dimensional form drag D_f can be expressed in term of the present nondimensional variables as

$$\frac{D_f}{\rho U^2 HL} = \int_{-\infty}^{\infty}\int_{-\infty}^{\infty} \psi(\partial\eta_B/\partial x)\, dydx$$

$$= \alpha^{-2}\int_{-\infty}^{\infty}\left[(a-b)(S_0+\frac{1}{2}sL_1)L_1 + (b-c)(S_0+\frac{1}{2}sL_2)L_2\right] d\mathcal{N} \qquad (4.12)$$

where the second step is obtained by substituting for ψ using (2.5) and performing the y-integration. For purely subcritical and supercritical states L_1 and L_2 are symmetric with respect to $\mathcal{N}$ and the integral in (4.12) vanishes. For critically-controlled flow L_1 and L_2 are asymmetric with respect to $\mathcal{N}$ and the integral is finite. Note further that the form drag is independent of the form of $\mathcal{N}(x)$ since no x-dependence is explicit in the integral.

Figure 5 contains a plot of form drag as a function of the maximum value of $s\mathcal{N}$ for the critically-controlled solutions having a–$b = 7$, b–$c = 1$, $\beta = s = S_0 = \alpha = 1$ and $L_1(-\infty) = 0$. The plot shows an approximately linear increase in form drag with $s\mathcal{N}_{max}$. Also shown are plots for a higher planetary potential vorticity gradient ($\beta = 2$) and lower inertial boundary layer thickness ($\alpha = 2$). In the first case the higher value of β

restricts the variations experienced by L_1 and L_2 and the form drag decreases. In the second case the larger β or smaller u_0 implied by larger $\alpha = (\beta/u_0)^{1/2}$ has a similar effect.

If the potential vorticity parameters a–b and b–c are known in addition to $L_2(-\infty)$ and ΔL_c, the form drag is uniquely determined as follows. Apply Eq. (4.3) to compute α and then use Figure 4 to determine Q. These complete the parameter set required to compute $L_1(\mathcal{N})$ and $L_2(\mathcal{N})$ and thus the form drag integral (4.12) can be calculated. In practice it might be possible to perform similar calculations to estimate the form drag of topographic features known to act as critical controls. The potential vorticity structure of the flow might be obtained from hydrographic sections taken upstream of the topography, and quantities like ΔL_c and $\Delta L_2(-\infty)$ might be obtained from satellite imagery. Of course this application will require the development of more sophisticated models.

5. Discussion

There are a number of geophysical flows to which the above model might apply. Armi (1989b) has argued that the winds of Jupiter may flow near the critical speed and may therefore be subject to upstream influence. More immediate applications might include midlatitude ocean jets such as the Gulf Stream and Kuroshio Extension. These currents are generally observed to spread (rather than narrow) in the downstream direction, although it is possible that local regions of narrowing might occur as topographic features like the Emperor and New England Seamounts are passed. However, there is little evidence of such narrowing and if critical control occurs, the control point may lie upstream where the flow runs along the western boundary (as suggested by Luyten and Stommel, 1985). In this case, the flow would be supercritical after separation from the coast and might resemble the super-to-subcritical solution shown in Figure 3.

A more likely candidate for critical control is the Antarctic Circumpolar Current (ACC) which appears to narrow across a number of topographic features. Evidence for this narrowing can be observed in the map of the 0–1000 db dynamic height anomaly appearing in the Gordon *et al.* (1986) atlas. For example, the 0.4 and 1.0 dynamic meter contours, which contain the greater part of the mass flux, experience a decrease in horizontal separation from 2500 km at 60E (slightly upstream of the Kerguelen Plateau) to 1400 km at 88E (slightly downstream of the Kerguelen Plateau). A second zone of convergence is observed between 130E and 170E where the contour separation narrows from 1600 to 800 km as the Macquarie Ridge is passed. A third possible choke point is the Drake Passage, although interpretation in terms of the dynamic height field is confused by the Falkland Current which drains water to the north.

It is well known (e.g., Nowlin and Clifford, 1982) that the ACC has a multi-front structure, the two most prominent features being the Subantarctic Front (SAF) and the Polar Front (PF). The largest eastward geostrophic velocities occur at the fronts and the flow thus has an element in common with the two-front model presented here.

In view of this similiarity, one might ask whether the necessary conditions (4.7) and (4.9) are satisfied by the ACC and what values of F_β occur. There is at least one conceptual obstacle to such a comparison, namely that the equivalent barotropic model assumes flow confined to a bottom layer underlying an inactive upper layer. In the ACC, on the other hand, the largest velocities generally occur in the upper water column. Thus, the critical parameters applicable to flow over the Kerguelen Plateau and Macquarie Ridge should be formulated using a more realistic representation of the stratification, perhaps through a two-layer model.

To obtain a preliminary estimate of F_β, one can treat the model as describing flow in an upper layer overlying an inactive lower layer. Since interaction with bottom topography is no longer possible, I set $\mathcal{N} = 0$ in the definition (4.8) of F_β and use the result to get an approximate indication of criticality of the flow. This approach is most valid in the vicinity of the Drake Passage, where the topographic forcing is primarily due to sidewall contractions. After inspection of the eleven sections appearing in the Gordon *et al.* (1986) atlas, it was found that the least ambiguous estimate of F_β possible is at section VIII (134W) where the ACC is relatively broad and is making its approach to the Drake passage. As an upper layer, the fluid between the 27.4 and 27.8 potential density surfaces is chosen. At 134W this layer ranges in depth from 200–700 m at 63S to 1300 to 2200 m at 54S. The width ΔL^* clearly corresponds to the distance between the SAF and PF, about 500 km at 134W. I do not attempt to estimate the value of u_0; rather, the inertial boundary layer thickness $(u_0^*/\beta^*)^{1/2}$ is simply taken as the observed decay scale of the geostrophic shear away from the two fronts. At 134W this scale is difficult to estimate but appears to lie within the range 60–250 km. Finally, the background potential vorticity difference $a^* - c^*$ is estimated by evaluating the stream function (Eq. 2.5) at y_a and y_c lying several $(u_0/\beta)^{1/2}$ units to the north of L_1 and south of L_2, respectively. These values give ψ (and hence the layer thickness) away from the region of strong horizontal shear. Subtracting the two expressions and converting to dimensional variables leads to

$$a^* - c^* = \beta^* H^{-1} \, (y_a^* - y_c^*) - g' f^{-1} H^{-1} \, (u_0^*/\beta^*)^{1/2} \, (H_a - H_c)$$

where H_a and H_c are the dimensional layer thickness at y_a^* and y_c^*. If y_a^* and y_c^* are chosen to be a distance $(u_0^*/\beta^*)^{1/2}$ to the north and south of the SAF and PF respectively, then $H_a = 880 \pm 50$ m and $H_c = 475 \pm 75$ m. Using these thicknesses and a mean thickness $H = 700$ m gives $a^* - c^*$ in the range $(1.7 \text{ to } 2.3) \cdot 10^{-8}$ m^{-1}s^{-1} for the given range in $(u_0^*/\beta^*)^{1/2}$.

Table 1 gives the values of F_β over the range of $(u_0^*/\beta^*)^{1/2}$ indicated above. Note that all values at 134W are <1 indicating subcritical flow. Also listed are the values of F_β corresponding to $\Delta L^* = 200$ km, which is typical of the frontal separation in the Drake Passage. Here F_β ranges from .38 to .90, with the majority of values lying between .81 and .90. Thus flow near the critical speed ($F = 1$) is indicated over most of the range of $(u_0^*/\beta^*)^{1/2}$. If the frontal separation is decreased again slightly, say to $\Delta L^* = 180$ km, the majority of F_β values exceed unity. Critical control by the Drake

Table 1. Estimates of F_β at 134W and 60W (Drake Passage) based on data from Gordon *et al.* (1986) and Nowlin and Clifford (1982).

$(u_0^*/\beta^*)^{1/2}$	F_β	
	$\Delta L^* = 500$ km (134W)	$\Delta L^* = 200$ km (Drake Passage)
60	2.6×10^{-3}	.38
90	2.0×10^{-2}	.56
120	6.7×10^{-2}	.81
150	0.12	.88
200	0.20	.90
250	0.27	.90

Passage would require $F_\beta < 1$ upstream, $F_\beta = 1$ at some point within, and $F_\beta > 1$ immediately downstream of the Passage. The downstream value of F_β is difficult to estimate due to the complexity of the flow field; however, given the uncertainties in the approximations and the simplicity of the model the above estimates within and upstream of the Passage are consistent with, if not suggestive of, critical control.

In the process of computing F_β it can be shown that $2\beta/\alpha(a - c) < 0.36$ so that (4.9) is satisfied. The other necessary condition (4.7) can be evaluated by estimating the volume flow rate Q^* contained between the SAF and PF and within the layer under consideration. Using Table 3 in Nowlin and Clifford (1982), I estimate $Q^* = (15 \pm 5)$ Sv, and this value must be less than $H^2\ (u_0^*/\beta^*)\ (a^* - c^*)$ in order that (4.7) be satisfied. Using the quantities calculated at 134W, the latter ranges from 90 to 625 Sv. The reader is reminded that (4.7) and (4.9) are necessary conditions for eastward flow in the model jet and their satisfaction is more an indication of model applicability than of critically-controlled flow.

In summary the frontal structure of the ACC allows comparison with the model developed herein, and satisfaction of (4.7) and (4.9) solidify the grounds for comparison. The streamline convergence over the Kerguelen Plateau and Macquarie Ridge is reminiscent of the critically-controlled solution of Figure 3. Although F_β is difficult to estimate at these locations, estimates at Drake Passage (a third possible control point) suggest flow near the critical speed. These estimates are based on the behavior of an individual density layer in which the PF and SAF are modeled as potential vorticity fronts. Refined estimates of F_β will require a model with more realistic stratification, perhaps allowing outcropping of density surfaces.

6. Conclusion

The calculations presented herein suggest that free jets in the ocean and atmosphere can be subject to the same upstream influence or control that occurs in fluid flow over a dam or through a nozzle. The implications of upstream influence are contained in Figure 4 showing that the flow rate Q^*, potential vorticity difference $(a^* - c^*)$, horizontal decay scale $(u_0^*/\beta^*)^{1/2}$ and thickness H of the jet cannot be specified

independently of the bottom topography when the flow is in a critically-controlled state. The topography thereby exercises influence over the general circulation as a whole, as opposed to exerting a purely local influence.

Along with the similarities with classical hydraulics, there are some important differences which should be pointed out. First, upstream influence in the jet is associated with potential vorticity waves having a varicose component; the gravity waves which exert upstream influence in free surface or internal hydraulics are irrelevant here. Also, the transition from supercritical to subcritical flow in a jet must be drastically different from the transition which occurs in classical hydraulics. In the latter case a hydraulic jump forms, in the former the constraints imposed by strong rotation may tend to suppress hydraulic jumps. In laboratory experiments with supercritical coastal currents in a strongly rotating environment Pratt (1987) showed that a lateral jump, characterized by an abrupt increase in the width of the current, can take the place of the classical hydraulic jump. Something akin may take place in a free jet; however, the question remains open.

Finally, it should be mentioned that hydraulic effects have apparently been observed by Rhines (1988) and Hogg (1988) in connection with models of broad, planetary-scale flows over ridges and other isolated obstacles. Their two-layer calculations based on the quasigeostrophic, planetary geostrophic models allow 0(1) changes in layer thicknesses. Familiar features such as blocking and critical flow are observed, but interpretation in terms of classical hydraulic phenomena is obscured by the full horizontal two-dimensionality of the flow field.

Acknowledgments. The author gratefully acknowledges the support of the National Science Foundation (Grant OCE-8700601) and the Office of Naval Research (Contract N00014-87-K-0007). Discussions with Professor Laurence Armi provided the initial impetus for the work and he suggested the Antarctic Circumpolar Current as a possible application. I would also like to thank Lisa Garner for typing the manuscript. This is Woods Hole Oceanographic Institution contribution number 6948.

REFERENCES

Armi, L. 1974. An energy minimization principal for oceanic currents and atmospheric jet streams. Geophys. Fluid Dyn. Notes, W.H.O.I. Ref. *74-63*(2), 1–14.

—— 1989a. Hydraulic control of zonal currents on a β-plane. J. Fluid Mech., (in press).

—— 1989b. Zonal currents: Application of an integral treatment to the westerlies of Jupiter, Saturn, Uranus and Earth. Icarus, (submitted).

Baines, P. G. and P. A. Davies. 1980. Laboratory studies in topographic effects in rotating and/or stratified fluids, *in* Orographic Effects in Planetary Flows. GARP Publ. *23*, World Meteorological Organization, Geneva, 1980, 233–299

Charney, J. G. 1955. The Gulf Stream as an inertial boundary layer. Proc. Nat. Acad. Sci., *41*, 731–740.

Clark, R. A. and N. P. Fofonoff. 1969. Oceanic flow over varying bottom topography, J. Mar. Res., *27*, 226–240.

Davey, M. K. 1980. A quasi-linear theory for rotating flow over topography. Part 1. Steady β-plane channel. J. Fluid Mech., *99*, 267–292.

Fofonoff, N. P. 1954. Steady flow in a frictionless homogeneous ocean. J. Mar. Res., *13,* 254–262.

Gill, A. E. and E. H. Schumann. 1979. Topographically induced changes in the structure of an inertial coastal jet: Application to the Agulhas Current. J. Phys. Oceanogr., *9,* 975–991.

Gordon, A. L., E. J. Malinelli and T. N. Baker. 1986. Southern Ocean Atlas, Columbia U. Press, 248 plates, 42 pp.

Hall, M. M. 1985. Horizontal and vertical structure of velocity, potential vorticity and energy in the Gulf Stream. Ph.D. thesis, Woods Hole Oceanographic, WHOI-85-16, 165 pp.

Hogg, N. G. 1988. Finite amplitude effects on deep planetary circulation over topography. J. Phys. Oceanogr., (submitted).

Hughes, R. L. 1979. On the dynamics of the equatorial undercurrent. Tellus *41,* 447–455.

—— 1981. On inertial instability of the equatorial undercurrent. Tellus, *33,* 291–300.

—— 1985. Multiple criticalities in coastal flows. Dyn. Atmos. Oceans, *9,* 321–340.

—— 1986. On the role of criticality in coastal flows over irregular bottom topography. Dyn. Atmos. Oceans, *10,* 129–147.

—— 1987. The role of higher shelf modes in coastal hydraulics. J. Mar. Res., *45,* 33–58.

Jacobs, S. J. 1964. On stratified flow over bottom topography. J. Mar. Res., *22,* 223–235.

Luyten, J. and H. Stommel. 1985. Upstream effects of the Gulf Stream on the structure of the mid-ocean thermocline. Prog. Oceanogr., *14,* 387–399.

McCartney, M. S. 1976. The interaction of zonal currents with topography with applications to the Southern Ocean. Deep-Sea Res., *23,* 413–427.

McIntyre, M. E. 1968. On stationary topography-induced Rossby-wave patterns in a barotropic zonal current. Deutsche Hydrograph. Zeitschrift, *21,* 203–214.

Merkine, Lee-Or. 1975. Steady finite-amplitude baroclinic flow over long topography in a rotating stratified atmosphere. J. Atmos. Sci., *32,* 1881–1893.

Nowlin, W. D. and M. Clifford. 1982. The kinematic and thermohaline zonation of the Antarctic Circumpolar Current at Drake Passage. J. Mar. Res. (Suppl), *40,* 481–507.

Pedlosky, J. 1987. Geophysical Fluid Dynamics. Springer-Verlag, 710 pp.

Pierrehumbert, R. T. 1985. Stratified semigeostrophic flow over two-dimensional topography in an unbounded atmosphere. J. Atmos. Sci., *42,* 523–526.

Pierrehumbert, R. T. and B. Wyman. 1985. Upstream effects of mesoscale mountains. J Atmos. Sci., *42,* 977–1003.

Porter, G. H. and M. Rattray. 1964. The influence of variable depth on steady zonal barotropic flow. Deutsche Hydrograp. Zeitschrift, *17,* 164–174.

Pratt, L. J. 1984. On nonlinear flow with multiple obstructions. J. Atmos. Sci., *41,* 1214–1225.

—— 1987. Rotating shocks in a separated laboratory channel flow. J. Phys. Oceanogr., *17,* 483–491.

Rhines, P. B. 1988. Deep planetary circulation and topography: Simple models of midocean flows. J. Phys. Oceanogr., (in press).

Robinson, A. R. 1960. On two-dimensional inertial flow in rotating stratified fluid. J. Fluid Mech., *9,* 321–332.

Stoker, J. J. 1957. Water Waves, Interscience, 567 pp.

Received: *27 May, 1988;* revised: *25 October, 1988.*